Ariel
IP: 139.140.112.4

3 **Rapid #: -2589199**

Status	Rapid Code	Branch Name	Start Date
Pending	LAF	Skillman Library	6/3/2009 10:10:42 AM

TYPE:	Article CC:CCL
JOURNAL TITLE:	Journal of microscopy
USER JOURNAL TITLE:	Journal of Microscopy
LAF CATALOG TITLE:	Journal of microscopy
ARTICLE TITLE:	Distribution of projection angles for single-axis-tilt electron microscope tomography of extended thin planar specimens.
ARTICLE AUTHOR:	Levy HA, Olins AL, Olins DE.
VOLUME:	165
ISSUE:	2
MONTH:	
YEAR:	1992
PAGES:	325-330
ISSN:	0022-2720
OCLC #:	1644311
CROSS REFERENCE ID:	140316
VERIFIED:	

BORROWER: **BBH :: Main Library**
PATRON: **Olins,Ada**

PATRON ID:	-
PATRON ADDRESS:	-
PATRON PHONE:	-
PATRON FAX:	-
PATRON E-MAIL:	-
PATRON DEPT:	Biology
PATRON STATUS:	Faculty
PATRON NOTES:	-

LAFAYETTE COLLEGE

Libraries and Information Technology Services

Interlibrary Loan (LAF)
710 Sullivan Road
Easton, PA 18042-1797
e-mail: ill@lafayette.edu

Phone: 610.330.5630
Fax: 610.252.0370
Ariel: 139.147.64.244
Odyssey: 206.107.42.51

PLEASE RETURN THIS COVER SHEET, ALONG WITH A COPY OF THE ORIGINAL REQUEST, IF THERE ARE ANY TRANSMITTAL OR COPY QUALITY PROBLEMS SUCH AS:

☐ Pages missing

Re-send pages: ____________________

☐ Edges cut off

Re-send pages: ____________________

☐ Illegible Copy – Re-send whole article

Reason:

☐ Too light

☐ Too dark

☐ Other (please explain) ____________________

☐ Wrong article sent

☐ Other (please explain) ____________________

OUR GOAL IS TO SERVE YOU BETTER!

Journal of Microscopy, *Vol.* 165, *Pt* 2, *February* 1992, *pp.* 325–330.
Received 12 *September* 1990; *revised* 22 *April* 1991; *accepted* 22 *May* 1991

Short Technical Note

Distribution of projection angles for single-axis-tilt electron microscope tomography of extended thin planar specimens

by HENRI A. LEVY, ADA L. OLINS* *and* DONALD E. OLINS*,
*Chemistry Division, and *The University of Tennessee-Oak Ridge Graduate School of Biomedical Sciences, and Biology Division, Oak Ridge National Laboratory, PO Box* 2009, *Oak Ridge, TN* 37831-8077, *U.S.A.*

KEY WORDS. Electron microscope tomography, three-dimensional reconstruction, projections on convex sets (POCS).

SUMMARY

An optimized distribution of tilt angles for tomography of specimens of non-circular cross-section is derived and tested with reconstructions of a phantom model.

INTRODUCTION

Projections uniformly distributed in tilt angle are usually employed in electron microscope tomography (Olins *et al.*, 1983; Sköglund & Daneholt, 1986; Frank, 1989). The expected resolution is given for specimens of circular cross-section by the formula of Crowther *et al.* (1970):

$$N = \pi D/d, \tag{1}$$

where D is the specimen diameter, d the resolution measure and N the number of uniformly distributed projections over the full 180° span. This expression is based on the extent of reciprocal space in which Fourier components of the reconstruction are properly defined by those of the projections.

When the specimen cross-section and consequently the reconstruction space is not circular, as is often the case in electron microscopy, the resolution becomes non-isotropic if the distribution of tilt angles remains uniform. In this note, we demonstrate that reconstructions are substantially improved if the distribution is optimized. A distribution somewhat similar to that presented here occurs in a different context in the 'concentric squares raster' reconstruction procedure (Mersereau & Oppenheim, 1974; this reference contains a comprehensive discussion of the field of reconstruction from projections).

DEVELOPMENT

Equation (1) may be recast to describe the non-circular case: π/N, the angular interval in radians between successive central sections, is replaced with $h(\alpha)$, and D becomes the projected reconstruction width at tilt angle α; the resolution measure d is then

$$d(\alpha) = h(\alpha)D(\alpha). \tag{2}$$

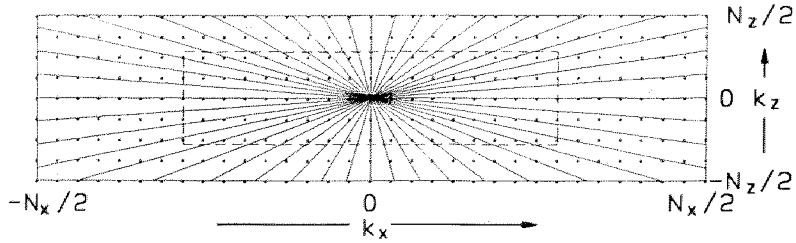

Fig. 1. Schematic illustration of the optimized distribution. The coordinate k_z is the Fourier space index across the thickness dimension of the planar section, and k_x is the index parallel to the section length. The dimensions, 32×8, and the number of tilts, twenty-three, are essentially one-quarter of those of the reconstructions shown in Figs. 2 and 3. Equation (2) yields the value 2·26 pixels for the nominal resolution d.

If $h(\alpha)$ is chosen to be inversely proportional to D, the equation predicts isotropic resolution. Equation (2) still requires central sections to span 180°; further modification would be needed to describe completely the resolution of incomplete spans. Like Eq. (1) this formula applies to non-iterative reconstructions in which no information beyond the observed projections is incorporated. Nevertheless it can serve as a guide to choosing proper tilt-angle distributions.

Justification of Eq. (2) with $h(\alpha) = c/D(\alpha)$ qualitatively follows the derivation of Eq. (1). The constant c defines the subarea of Fourier reconstruction space for which all coefficients are reliably determined by those of the observed projections. Thus the corresponding central sections must be distributed within this subarea to fall close to the raster of coefficients which defines the reconstruction. Since the angular interval between adjacent raster points is inversely proportional to D, the projections should also be so distributed.

In this presentation, the reconstruction space is rectangular, as is appropriate for extended electron micrograph sections, and is also correct for use of the fast Fourier transform (FFT) algorithm. The rationale is illustrated in Fig. 1, which shows a 32×8 grid in reciprocal space whose values are the Fourier components of the reconstruction. Superposed is a set of twenty-three central sections chosen according to Eq. (2) with $h = c/D$. The proportionality constant c is a function of the number of tilt angles, the maximum tilt angle and the dimensions of the reconstructed area; its value was established by an iterative algorithm to yield the desired values. A *FORTRAN* subroutine for the computation is shown opposite.

The equations for h are a linearized solution, valid for small h, of the expression $h(\alpha_i) = c/D(\alpha_{i-1} + h/2)$, which assigns h to the midpoint of interval i. The central sections are most closely spaced near the diagonal where the projection width is greatest. The inner rectangle, whose dimensions are proportional to those of the full grid, is drawn so that the length of the semi-perimeter is equal to the number of central sections; thus every grid point within this rectangle lies close to one of the central sections.

As a part of an ongoing study of various reconstruction techniques for electron microscope tomography, we have examined reconstructions employing this optimized distribution. The phantom for the study consisted of a 128×32 pixel rectangle from a digitized electron micrograph, in order to approximate actual data. This phantom was embedded in a null space of dimensions 1024×256 and Fourier transformed. Central sections of this eightfold interpolated transform were extracted to serve as Fourier-transformed projections for the reconstructions.

The reconstruction technique used was projections on convex sets (POCS) (see, for example, Carazo & Carrascosa, 1987). Conditions imposed on the POCS procedure were (i) agreement with the 'observed' central sections in Fourier space, and, in direct

```
      SUBROUTINE ANGLES(TILTS,NTLT,TLTM,NX,NZ)
C       A subroutine to generate tilt angles at intervals inversely
C     proportional to projected width of a rectangular reconstruction
C     space with width NX and thickness NZ.
C       NTLT=desired number of tilt angles.
C       TLTM=desired maximum tilt angle (Degrees). TLTM.GE.ATAN(NZ/NX).
C       TILTS(1) is defined to be zero degrees.
C       Positive and negative tilt angles alternate in the array.
      DIMENSION TILTS(NTLT)
      DATA DEG/0.01745352925/
      FNX=NX
      FNZ=NZ
      TLTC=ATAN(FNZ/FNX)/DEG
      HOLD=TLTM*DEG
      COSTM=COS(HOLD)
      SINTM=SIN(HOLD)
      TILTS(1)=0.
      CSAV=0.
      TSAV=0.
C       Estimate an initial value for C.
      C=0.6*(FNX+FNZ-FNZ*COSTM/SINTM)/FLOAT(NTLT-1)
C       Compute the tilt values.
   25 DO 30 I=2,NTLT,2
        TLT=-TILTS(I-1)
        ANG=TLT*DEG
        COST=COS(ANG)
        SINT=SIN(ANG)
        IF (TLT.LE.TLTC) THEN
          H=(2.*C*COST)/(FNX+C*SINT)
        ELSE
          H=(2.*C*SINT)/(FNX-C*COST)
        END IF
        TILTS(I)=TLT+H/DEG
        TILTS(I+1)=-TILTS(I)
   30 CONTINUE
C       Accept the values of TILTS if the computed maximum is
C     within tolerance of the desired value.
      TMX=TILTS(NTLT-1)
      IF(ABS(TMX-TLTM).LE.0.04) GOTO 35
C       Otherwise, iterate with a refined value for C.
      CNEW=CSAV+(C-CSAV)*(TLTM-TSAV)/(TMX-TSAV)
      CSAV=C
      C=CNEW
      TSAV=TMX
      GOTO 25
   35 RETURN
      END
```

space, (ii) non-negative density inside, and (iii) zero density outside the reconstructed specimen boundaries.

The quality of the reconstruction was evaluated by computing and displaying the Fourier transform of $R \cdot P^*/P \cdot P^*$, where R and P are the Fourier transform components of the reconstruction and phantom, respectively, and the asterisk signifies the complex conjugate. This function is analogous to the point-spread or convolution function associated with a filter; when convolved with the phantom, it yields the reconstruction. For a perfect reconstruction, the function is unity at the origin and zero elsewhere. Although a valid indicator of overall quality, this function should not be interpreted as a true point-spread, as it is not necessarily position independent in the present context.

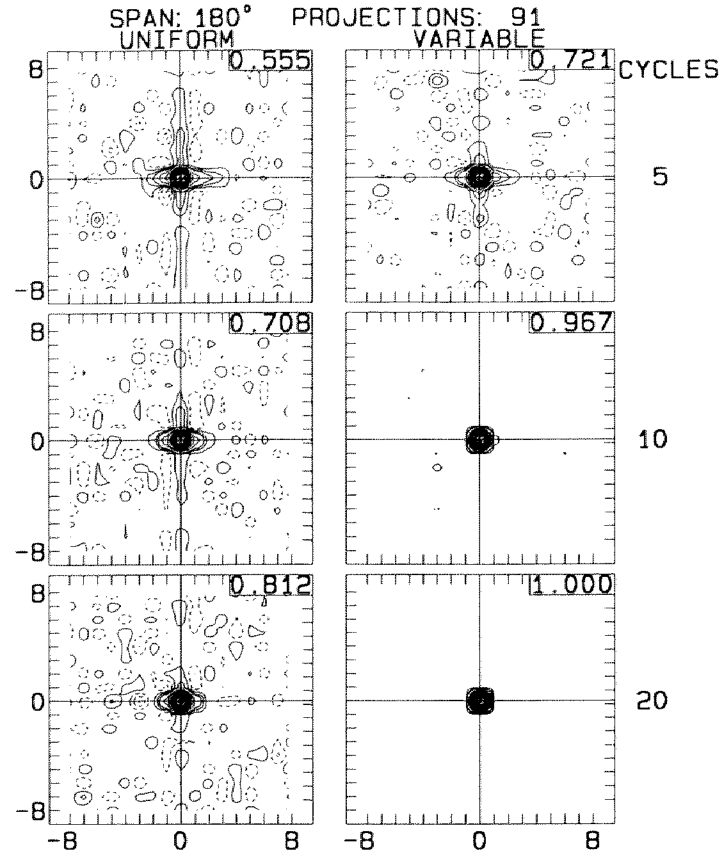

Fig. 2. Central region of 'point-spread functions' for reconstructions of a planar phantom with ninety-one tilts covering a complete 180° span: left, uniformly distributed tilts; right, optimized variably distributed tilts, for representative projection on convex sets (POCS) iterations.

RESULTS

Figure 2 shows the central region of 'point-spread functions' for reconstructions with ninety-one projections spanning 180° tilt, for both uniform and variable distributions, as a function of POCS iteration. The peak value at the origin is given for each distribution. The superiority of the optimized distribution is evident by visual comparison of peak values, peak asymmetry and surrounding noise levels at each iteration.

Figure 3 shows corresponding functions for data limited by a maximum tilt angle of 60°, a typical limitation imposed in practice by the design of commercially available tilt stages as well as by excessively large effective specimen thickness at high tilt angles. Again the superiority of the optimized distribution of tilt angles is evident. Some characteristics of these reconstructions are given in Table 1.

Figure 4 presents the origin peak values of the point-spread functions as POCS iteration proceeds. The power of the optimized distribution of projections applied with POCS iteration is demonstrated by the equally good or somewhat superior results obtained with the variable 61-tilt, 120° incomplete-span reconstruction compared to those obtained with ninety-one uniformly distributed tilts covering the complete span of 180°.

DISCUSSION

Our results indicate that substantial improvement in reconstruction quality can be

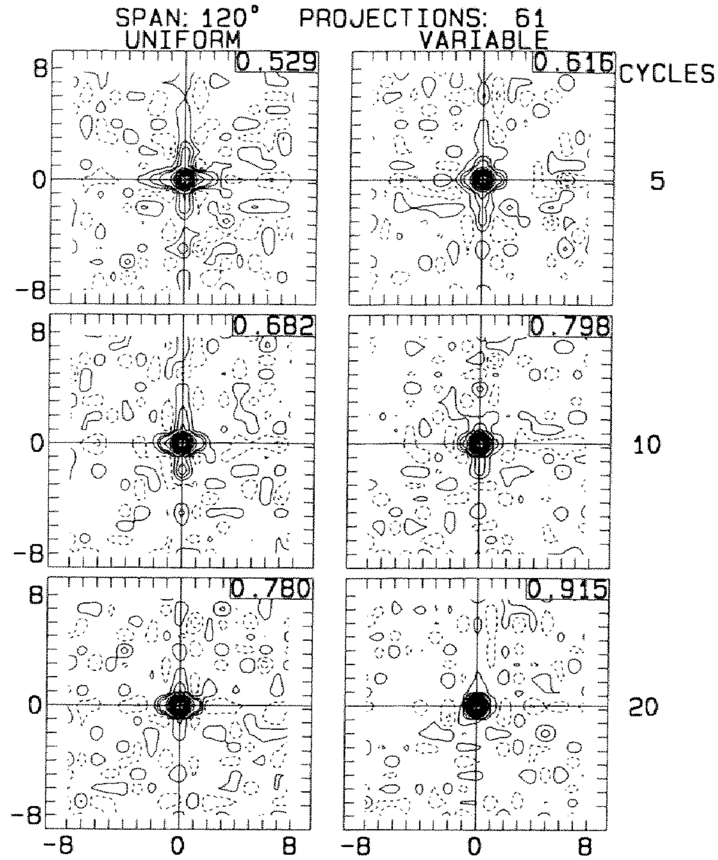

Fig. 3. Similar to Fig. 2, for sixty-one tilts covering a span of 120°.

achieved with the optimized distribution of tilt angles. The optimized distribution derived here depends on the dimensions of the reconstructed area of the specimen. In practice, projections are measured on specimens of essentially unlimited length. Thus the measured projections should be masked to yield approximations to those of limited length appropriate to the reconstruction. We are examining masking methods and their effect on reconstruction quality as part of our present study.

The use of central sections extracted from the Fourier transform of the phantom limits this study to the effects of the limited angle distribution. Absent are effects of finite resolution in the observed projections and of errors arising in the assignment of

Table 1. Some characteristics of the reconstructions.

Tilts	Span	Average	Tilt interval Max.	Tilt interval Min.	d* at tilt 0°	d* at tilt 14·04°	d* at tilt 60°	d* at tilt 90°
91 var.	180°	2·00°	3·93°	0·95°	2·19	2·19	2·19	2·19
91 unif.	180°	2·00°	2·00°	2·00°	4·47	4·60	2·58	1·12
61 var.	120°	2·00°	4·11°	1·17°	2·70	2·70	2·70	2·70
61 unif.	120°	2·00°	2·00°	2·00°	4·47	4·60	2·58	—

* The nominal measure of resolution d in pixels as given by Eq. (2). The angle 14·04° is that of the diagonal of the rectangle where the tilt interval is a minimum.

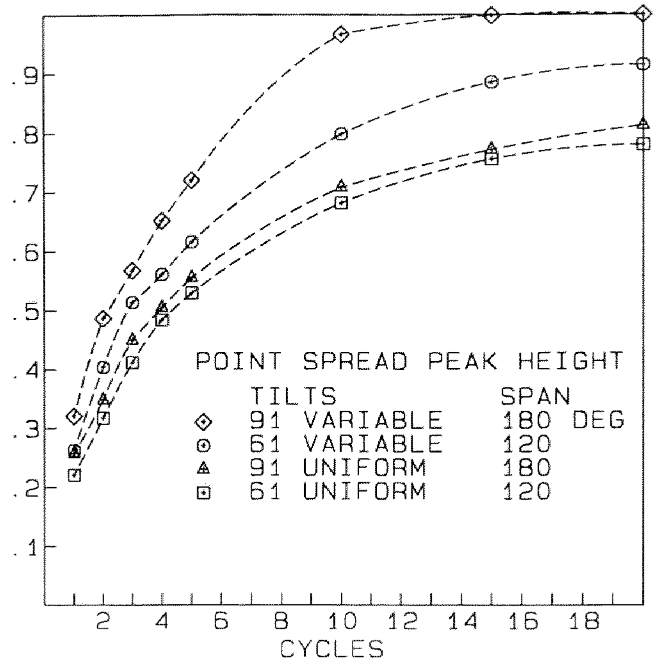

Fig. 4. Plots of 'point-spread function' origin peak height versus projection on convex sets (POCS) iteration number.

their Fourier components to the two-dimensional Fourier space array in the reconstruction process.

Application of the optimized distribution requires knowledge of the length-to-thickness ratio of the desired reconstruction space before final projection data are collected. Thus a preliminary examination of the specimen is necessary. Such an estimate can be made from observation of the motion of surface features of the specimen, e.g. adsorbed colloidal particles, when the specimen is tilted through a small angle.

ACKNOWLEDGMENTS

We are grateful to our colleagues Edward C. Uberbacher and Manesh Shah for valuable discussions of the problems underlying this work, and for a critical reading of this manuscript. This study was funded by NSF DIR8700518 and the Office of Health and Environmental Research, the U.S. Department of Energy, under contract DE-AC05-840R21400 with the Martin Marietta Energy Systems, Inc.

REFERENCES

Carazo, J.M. & Carrascosa, J.L. (1987) Information recovery in missing angular data cases: an approach by the convex projections method in three dimensions. *J. Microsc.* **145**, 23–43.

Crowther, R.A., DeRosier, D.J. & Klug, A. (1970) The reconstruction of a three-dimensional structure from projections and its application to electron microscopy. *Proc. Roy. Soc. Lond. A*, **317**, 319–340.

Frank, J. (1989) Three-dimensional imaging techniques in electron microscopy. *BioTechniques*, **7**, 164–173.

Mersereau, R.M. & Oppenheim, A.V. (1974) Digital reconstruction of multidimensional signals from their projections. *Proc. IEEE*, **62**, 1319–1338.

Olins, D.E., Olins, A.L., Levy, H.A., Durfee, R.C., Margle, S.M., Tinnel, E.P. & Dover, S.D. (1983) Electron microscope tomography: transcription in 3-D. *Science*, **220**, 498–500.

Sköglund, U. & Daneholt, B. (1986) Electron microscope tomography. *Trends Biochem. Sci.* **11**, 499–503.